# Calcium phosphate formation on nanocrystalline $ZrO_2$ thin film prepared by using a zirconium naphthenate

KYU-SEOG HWANG*, YEON-HUM YUN, BO-AN KANG, SANG-BOK KIM, SEUNG-WOOK JANG, CHI-KYOON KIM
*School of Automotive and Mechanical Engineering and Institute of Manufacturing and Automation System, Nambu University, 864-1 Wolgye-dong, Gwangsan-gu, Gwangju 506-824, South Korea*
*E-mail: khwang@mail.nambu.ac.kr*

JEONG-SUN OH
*Department of Chemistry, College of Natural Science, Chosun University, 375 Seosuk-dong, Dong-gu, Gwangju 501-759, South Korea*

To investigate the calcium phosphate forming ability of $ZrO_2$ thin film, we prepared $ZrO_2$/Si structure by a chemical solution deposition with a zirconium naphthenate as a starting material. Precursor sol was spin-coated onto the cleaned Si substrate and prefired at 500 °C for 10 min in air, followed by final annealing at 800 °C for 30 min in air. Surface morphology and surface roughness of the annealed layer were characterized by field emission-scanning electron microscope and atomic force microscope. After soaking for 5 days in a simulated body fluid, formation of the calcium phosphate on nanocrystalline $ZrO_2$ layer annealed at 800 °C was observed by energy dispersive X-ray spectrometer. Fourier transform infrared spectroscopy revealed that carbonate was substituted into the calcium phosphate.


## 1. Introduction

Among various techniques to prepare oxide thin films, chemical solution processes such as sol–gel and dipping-pyrolysis, have several advantages: ease of chemical composition control, high purity, low-temperature processing, applicability to substrates with any size and shape, etc [1–5]. A wet chemical solution deposition (CSD) has successfully been used to prepare oxide films [6, 7].

Among various bioceramics, zirconia ($ZrO_2$) has long been a candidate biomaterial that could possibly replace titanium in selected mechanically and chemically demanding tissue applications, such as dental restorations [8]. Some previous works showed that apatite was successfully deposited on $ZrO_2$ ceramics [9, 10]. Similar to the formation of calcium phosphate (CaP) on the surfaces of oxide films such as titanium and silica [11, 12], if $ZrO_2$ is produced in the form of coating on implants surfaces, which corresponds to the ZrOH formation, its advantages can be properly exploited, since it was suggested that a surface hydroxyl group as well as surface structure with a high surface area was formed showing markedly improved surface wettability, which might play an important role in the CaP forming ability in a simulated body fluid (SBF). However, until now, there has been little information on the bioactivity of chemical solution derived $ZrO_2$ thin film by using a metal naphthenate as a starting material.

Metal naphthenates are more advantageous than metal alkoxides as starting materials, in terms of cost, stability in air and ease of handling. Preparation of coating solution using zirconium naphthenate was easily performed by the addition of toluene, while complicated procedure was needed for the preparation of sol by using zirconium alkoxide. Furthermore, it should be noted that vaporization of the additives, such as alcohol, water and catalyst etc, during prefiring and annealing might cause unwanted cracks and pores in the coating. On the other hand, in our paper, prefiring is the process for pyrolytic conversion of zirconium naphthenate into $ZrO_2$, while the final annealing is the process for solid-state reaction. In our previous works [2, 13] by using metal naphthenates, it was observed that the annealed films were smooth and it was difficult to identify cracks and pores, while defects were easily observed at the surface of metal alkoxide derived layers. In biological applications, the partially deteriorated layer may present some disadvantages, such as delamination and fracture at the film-implant interface.

In this work, in order to use chemical solution derived $ZrO_2$ films with a zirconium naphthenate as the driving site for CaP formation and high strength and fracture

*Author to whom all correspondence should be addressed.

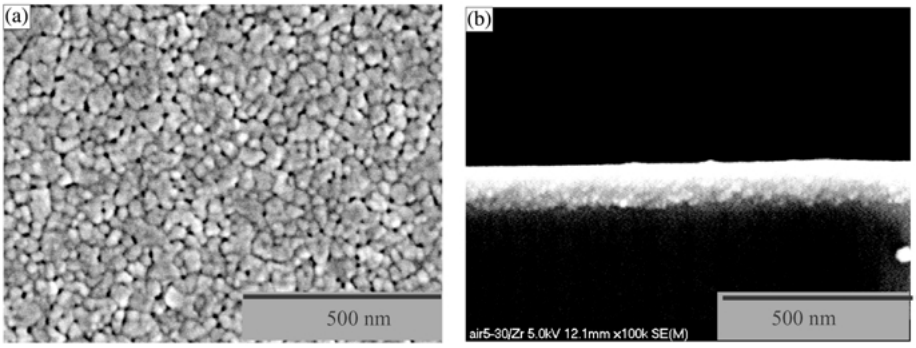


*Figure 1* FE-SEM images of free surface (a) and fractured-cross section (b) of $ZrO_2$/Si after annealing at 800 °C.

toughness of $ZrO_2$, the formation of CaP after immersing the $ZrO_2$ films in SBF was investigated.

## 2. Experimental procedure

Metal naphthenates which consist of cyclopentanes or cyclohexanes, methylene chains, carboxylates and metals mainly have the following structure:

$$[(\text{cyclopentane})\text{–}(CH_2)_n\text{–}COO]_m^- \text{–} M^{m+}$$

They were stable in air and sticky liquids at room temperature.

A coating solution was prepared using zirconium naphthenate (Nihon Kagaku Sangyo Co., Ltd., Japan) and by diluting the solution with toluene (concentration: 0.037 g metal/ml coating solution) to achieve an appropriate viscosity for the deposition of smooth and crack-free films.

Si-wafer (1 0 0) was selected as a substrate. To remove organics and contaminants attached on Si, the substrate was cleaned in acetone, immersed in $H_2O_2$ solution and rinsed in toluene. Before coating, to avoid nonstoichiometry of the coating layer probably due to oxygen diffusion from $ZrO_2$ film to Si substrate during high temperature annealing, $SiO_2$ thin film as a buffer layer was formed by a thermal oxidation of the cleaned Si substrate at 500 °C for 10 min in air.

Pre-annealed substrates were spin-coated with the dropping solution at 1500 rpm for 10 s and pyrolyzed at 500 °C for 10 min in air in order to vaporize organics. The spin coating and pyrolysis were performed three times to adjust the thickness of the precursor films. To make nano-crystalline $ZrO_2$ layer with high surface area, these pyrolyzed precursor films were finally annealed at 800 °C for 30 min in air (flow rate: 150 ml/min) by directly inserting the samples into a preheated furnace, which was followed by fast cooling.

The surface morphology and the surface roughness of the annealed films were observed by a field emission-scanning electron microscope (FE-SEM, S-4700, Hitachi, Japan) and an atomic force microscope (AFM, Nanoscope Multimodel SPM, SPM-Digital Instruments, USA). All the AFM measurements were performed in air using the tapping mode with silicon probes having a $\sim$ 260 kHz resonant frequency.

The *in vitro* formation of CaP was evaluated by immersing the annealed samples in 15 ml SBF for 5 days. The SBF was prepared by dissolving NaCl, $NaHCO_3$, KCl, $K_2HPO_4 \cdot 3H_2O$, $MgCl_2 \cdot 6H_2O$, $CaCl_2$ and $Na_2SO_4$ in deionized water. To this solution, 50 mM tris-(hydroxymethyl) aminomethane $[(CH_2OCH_3)CNH_2]$ and 45 mM hydrochloric acid (HCl) were used as buffering agents to maintain the pH of SBF at 7.25 at 36.5 °C [14]. The reagent-grade chemicals were used and their concentration for the preparation of SBF are shown in Table I.

The *in-vitro* test was performed in a constant temperature-circulating bath (Model 90, Poly Science, USA) at a temperature of 36.5 °C. After immersion for 1 or 5 days, the samples were removed from the SBF, carefully rinsed with distilled water, and dried at room temperature.

The morphology and composition of the surface of the immersed samples were evaluated using FE-SEM equipped with an energy dispersive X-ray spectrometer (EDX) that has a Robinson type back-scattered electron detector. Fourier transform infrared (FTIR) spectroscopy (FTS-60, BIO-RAD Digilab, USA) in transmission mode with 4 $cm^{-1}$ resolution was chosen to monitor the spectral evolution of chemical bonding of CaP on $ZrO_2$.

## 3. Results and discussion

The surface morphology and fractured-cross section of the $ZrO_2$ film was examined by FE-SEM. Fig. 1(a) and (b) show FE-SEM photographs of the free surface and cross section of film, respectively. The free surfaces of the $ZrO_2$ film show circular grains. The morphology of the film was similar to typical polycrystalline films prepared by general metal–organic deposition [1, 3]. Fracture surface of the $ZrO_2$ film on Si was uniform and dense along the cross-section direction (film thickness = $\sim$ 0.13 μm), in Fig. 1(b).

TABLE I Regents for preparing the SBF

| Reagents | Amount g/l $H_2O$ |
|---|---|
| $(CH_2OH)_3CNH_2$ | 6.055 |
| NaCl | 7.995 |
| $NaHCO_3$ | 0.353 |
| KCl | 0.224 |
| $K_2HPO_4 \cdot 3H_2O$ | 0.228 |
| $MgCl_2 \cdot 6H_2O$ | 0.305 |
| $CaCl_2 \cdot 2H_2O$ | 0.368 |
| $Na_2SO_4$ | 0.071 |
| 2 mol/l HCl | 20 mL |

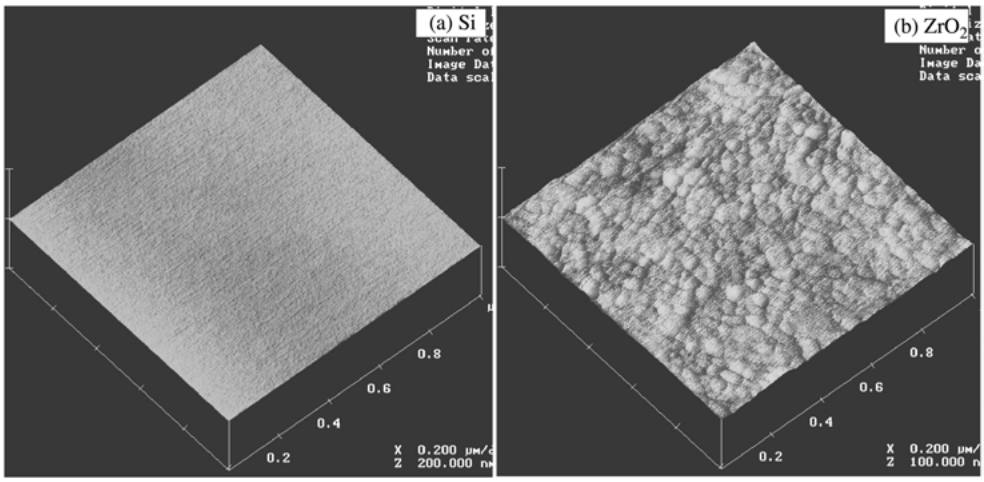


*Figure 2* AFM images of (1 0 0) Si substrate and $ZrO_2$ after annealing at 800 °C.

In order to elucidate the surface roughness and morphology of the film after annealing, AFM analysis was performed. Fig. 2 shows the AFM images of the surface of Si substrate and $ZrO_2$ thin film after annealing at 800 °C. The smoothness of the surface of (1 0 0) Si is very high. Based on AFM scans of $1 \times 1\,\mu m^2$, the grain size mean of $ZrO_2$ thin film after annealing at 800 °C is estimated to be around $6.2\,nm^2$.

Fig. 3 shows AFM top-view images and surface roughness profiles of (100) Si and $ZrO_2$ thin film annealed at 800 °C. Film after annealing showed much higher root mean square (RMS) roughness than that of the Si substrate, as shown in Fig. 3. In this case, we conclude that surface roughness of the film may be increased by grain growth of $ZrO_2$ during annealing, resulting in the increase in RMS roughness.

Further, we studied the surface roughness characteristics of nano-crystalline $ZrO_2$ layer using power spectral density (PSD) curves obtained from AFM measurement. To investigate a larger PSD data, PSD curves obtained from combined AFM results, which were recorded over scan area from $0.1\,\mu m \times 0.1\,\mu m$ and $1\,\mu m \times 1\,\mu m$ to $10\,\mu m \times 10\,\mu m$, were presented. When one evaluates the surface roughness, the PSD function is used increasingly as a valuable tool for topography description at surfaces. For a randomly rough surface such as chemical solution derived films, many different spatial frequencies are present. This is quantitatively expressed by the PSD curve, giving the relative strength of each roughness component of a surface microstructure as a function of the spatial frequency [7], whereas the RMS roughness as a single parameter of surface description reflects the standard deviation of all height values within the considered surface and does not provide any information on the topographical details of the surface.

Fig. 4 shows the result of PSD functions for the Si substrate (a) and $ZrO_2$ layer (b). Similar to that of Si, the PSD function of the $ZrO_2$ layer displays no inflated shape generally due to increase in grain size. In addition, PSD curve with a gentle grade indicating that the layer

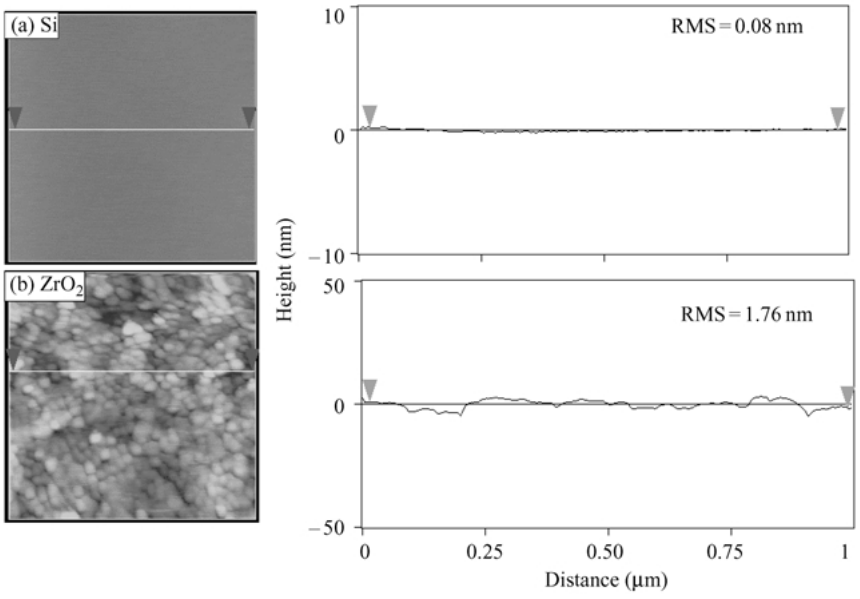


*Figure 3* AFM top-view images and surface roughness profiles of (1 0 0) Si and $ZrO_2$ thin film annealed at 800 °C.

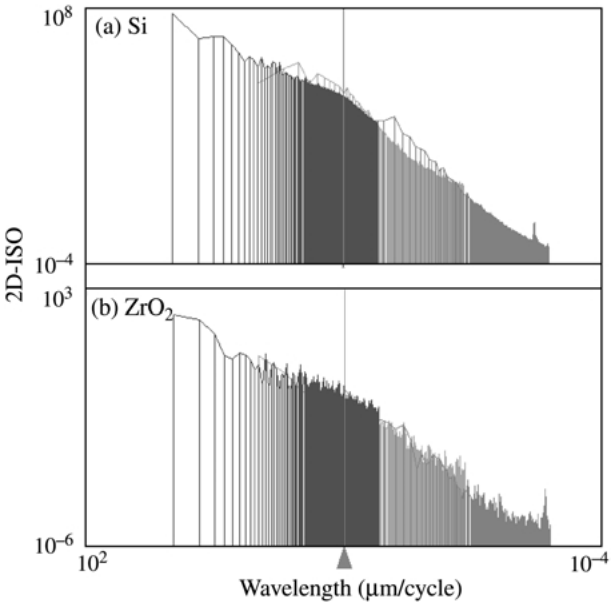


*Figure 4* PSD curves of Si (a) and $ZrO_2$ thin film (b).

structure has grown uniformly both in height and width (see Fig. 4(b)).

FE-SEM and EDX analysis were performed on the samples after immersion for 1 day (Fig. 5(a)) and 5 days (Fig. 5(b)). As shown in Fig. 5(a), partially adsorbed crystals on $ZrO_2$ film were identified after immersion for 1 day. As increase with the immersing time to 5 days, surface of the $ZrO_2$ film was wholly covered with CaP as well as relatively small amounts of other ions such as Na, Cl and Mg.

The calcium and phosphate ions required for hydroxy apatite generation on the film surface were derived from the SBF. This was indicated by an increase of the formation of CaP on $ZrO_2$ (see Fig. 5(a) and (b)). As clearly shown in Fig. 5(a) and (b), the $ZrO_2$ film with nano-sized crystals with higher surface area and roughness than those of Si substrate showed a high CaP forming ability.

The first step in the nucleation of hydroxy apatite in the presence of an osteoconductive oxide is thought to be an electrostatically driven adsorption of $Ca^{2+}$ ions at ionized surface hydroxyl groups onto which phosphate is subsequently adsorbed [15].

Compared to a micro- or macro-crystalline oxide film in solution, a nanocrystalline surface is more open for ions to be incorporated. Moreover, from an electrostatic interaction point of view, surface hydroxyl groups present on or inside the oxide layer tend to attract calcium ions from the solution [16].

In our work, a newly formed nanocrystalline $ZrO_2$ layer with a high surface area was probably responsible for CaP forming ability of $ZrO_2$ thin film.

In order to confirm the structure of the CaP layer, we performed FTIR analysis, as shown in Figs. 6 and 7. FTIR measurement showed distinct $v_3$ (at around 1050 and 1100 $cm^{-1}$) and $v_4$ (at 600 and 570 $cm^{-1}$) phosphate ($PO_4^{3-}$) spectral bands.

As summarized by previous works [17, 18], the carbonate ions occupy two different sites: band at 874 $cm^{-1}$ is due to the $v_2$ vibrational mode, and bands at 1419 and 1455 $cm^{-1}$ are due to $v_3$ vibrational mode carbonate ion. As shown in Fig. 6, the characteristic peaks of carbonated apatite are seen in the spectra, $CO_3^{2-}$ $v_2$ at 870–875 $cm^{-1}$ and $CO_3^{2-}$ $v_3$ at 1400–1450 $cm^{-1}$.

The carbonate apatite is known to exist in three different forms: In the A type, the carbonate is located at monovalent anionic $OH^-$ sites; in the B type carbonate is at trivalent phosphate ($PO_4^{3-}$) sites; and in the third form, the carbonate is at labile environment sites of hydroxy apatite $Ca_{10}(PO_4)_6(OH)_2$ [11]. In the biological apatites two sets of corresponding bands have been reported for the A type 1545, 1450, and 890 $cm^{-1}$ and for the B type 1465, 1412 and 873 $cm^{-1}$ [19]. From our FTIR results as shown in Figs. 6 and 7, it seems that B-type carbonates formed on the $ZrO_2$ surfaces after *in vitro* SBF test.

Furthermore, the broad peak that appeared at 1650 $cm^{-1}$ was assigned to physically adsorbed OH. Although SBF is supersaturated with respect to apatite [20], it is metastable because of the high energy required to form critical nuclei and the presence of inhibitors like $Mg^{2+}$. However, titania and silica gel prepared by sol–gel method can act as a stimulant to induce

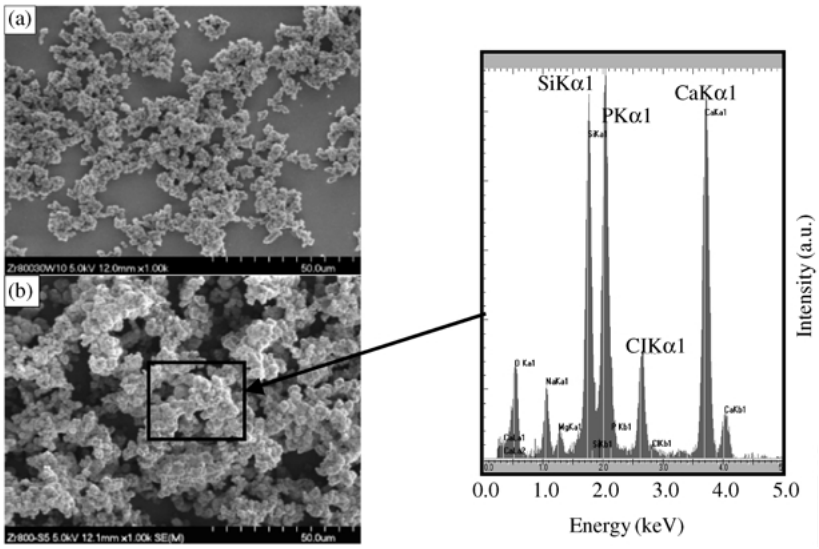


*Figure 5* FE-SEM and EDX analyses of the samples after immersion for 1 day (a) and 5 days (b) in SBF.

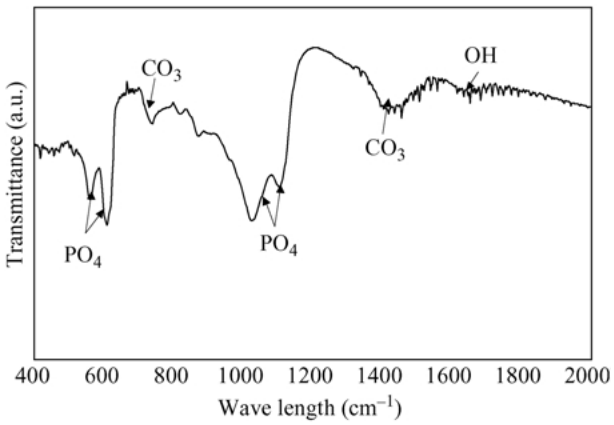


*Figure 6* FTIR spectra of the samples after immersion for 5 days in SBF.

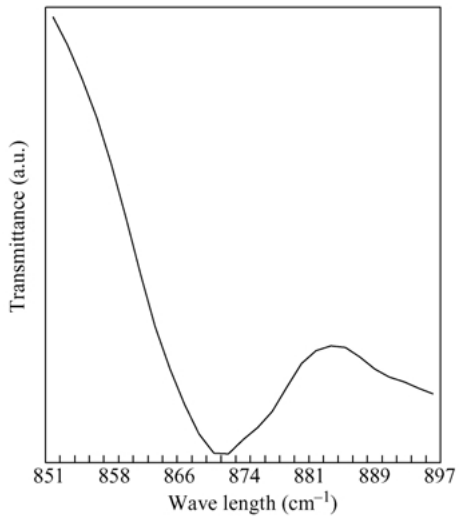


*Figure 7* Magnified FTIR spectra of the samples after immersion for 5 days in SBF.

hydroxyapatite heterogeneous nucleation. Once apatite nuclei form, they grow spontaneously by taking the calcium and phosphate from SBF [14]. Certain hydroxyl groups, such as SiOH and TiOH, remaining in the sol–gel-prepared materials or absorbing during storage and immersion appear to promote hydroxyapatite generation by providing the sites for the CaP nucleation [12, 14, 21]. Furthermore, Peltola *et al*. [11] suggested that increasing the sintering temperature from 400 to 600 °C decreases the amount of TiOH groups. Ti-gels annealed at 500 °C formed hydroxyapatite on their surface the fastest of all coatings in their study. On the other hand, Cho *et al*. [14] suggested that the SiOH groups newly formed on the surface of the silica gel treated at below 800 °C by immersing in SBF could be responsible for hydroxyapatite nucleation.

Although, further experimental study is still needed for identifying a forming period of ZrOH groups, the results of the present work suggest that $ZrO_2$ thin film, when using the CSD with a zirconium naphthenate, with nano-sized crystals and ZrOH groups may exhibit a CaP forming ability in SBF.

## 4. Summary

The successful production of bioactive $ZrO_2$ thin film on Si substrate has been demonstrated using a CSD with a zirconium naphthenate as a starting material. By AFM observation, $ZrO_2$ thin film after annealing at 800 °C showed much higher surface area and RMS roughness than those of Si substrate. In order to examine osteoconductivity, annealed films were immersed in SBF for 5 days. As confirmed by FE-SEM and EDX analyses, samples annealed at 800 °C with nano-scaled crystals showed high CaP forming ability. B-type carbonate apatite formation at the surface of $ZrO_2$ layer was confirmed by FTIR.

## Acknowledgment

This work was supported by the Korean Research Foundation Grant (KRF-2002-041-D00593).

## References

1. K. S. HWANG, H. M. LEE and Y. M. LIM, *J. Mater. Sci.* **35** (2000) 6209.
2. K. S. HWANG and Y. J. PARK, *J. Mater. Res.* **16** (2001) 2519.
3. K. S. HWANG, S. S. MIN and Y. J. PARK, *Surf. Coat. Tech.* **137** (2001) 205.
4. K. S. HWANG, Y. H. YUN, B. A. KANG and Y. H. KIM, *J. Mater. Sci.* **37** (2002) 365.
5. K. S. HWANG, H. A. PARK, B. S. JUNG, B. A. KANG and Y. H. KIM, *J. Sol–Gel Sci. Technol.* **23** (2002) 67.
6. K. S. HWANG, C. K. KIM, S. B. KIM, J. T. KWON, J. S. LEE and Y. H. YUN, *Surf. Coat. Tech.* **150** (2002) 177.
7. K. S. HWANG, Y. H. YUN, H. W. RYU and B. A. KANG, *Jpn. J. Appl. Phys.* **41** (2002) 795.
8. S. F. HULBERT, in ''An Introduction to Bioceramics'', edited by L. L. Hench and J. Wilson (World Scientific, Singapore, 1993) pp. 25–40.
9. S. NAKAMURA and K. YAMASHITA, *Key Eng. Mater.* **218–220** (2002) 661.
10. N. KAWASHIMA, K. SOETANO, K. WATANABE, K. ONO and T. MATSUNO, *Colloids Surf. B* **10** (1997) 23.
11. T. PELTOLA, M. PÄTSI, H. RAHIALA, I. KANGASNIEMI and A. YLI-YRPO, *J. Biomed. Mater. Res.* **41** (1998) 504.
12. P. LI, C. OHTSUKI, T. KOKUBO, K. NAKANISHI, N. SOGA and K. DE GROOT, *ibid.* **28** (1994) 7.
13. K. S. HWANG, T. MANABE, T. NAGAHAMA, I. YAMAGUCHI, T. KUMAGAI and S. MIZUTA, *Thin Solid Films* **347** (1999) 106.
14. S. B. CHO, K. NAKANISHI, T. KOKUBO, N. SOGA, C. OHTSUKI, T. NAKAMURA, T. KITSUGI and T. YAMAMURO, *J. Am. Ceram. Soc.* **78**(7) (1995) 1769.
15. B. C. YANG, J. WENG, X. D. LI and X. D. ZHANG, *J. Biomed. Mater. Res.* **47** (1999) 213.
16. J. PAN, H. LIAO, C. LEYGRAF, D. THIERRY and J. LI, *ibid.* **40** (1998) 244.
17. J. BARRALET, S. BEST and W. BONEFIELD, *ibid.* **41** (1998) 79.
18. M. VIGMOLES, G. BONEL, D. W. HOLCOMB and R. A. YOUNG, *Calcif. Tiss. Int.* **43** (1988) 33.
19. C. REY, B. COLLINS, T. GOEHL, I. R. DICKSON and M. J. GILMCHER, *ibid.* **45** (1989) 157.
20. C. OHTSUKI, T. KOKUBO and T. YAMAMURO, *J. Non-Cryst. Solids* **143** (1992) 84.
21. P. LI, K. DE GROOT and T. KOKUBO, *J. Am. Ceram. Soc.* **77** (1994) 1307.

*Received 29 July*
*and accepted 23 December 2002*